Generation of near-Earth reconnection by divergent flows in the plasma sheet

Y. Lin
Physics Department, Auburn University, Auburn, Alabama, USA

D. W. Swift
Geophysical Institute, University of Alaska, Fairbanks, Alaska, USA

Received 4 February 2002; revised 24 June 2002; accepted 21 August 2002; published 16 November 2002.

[1] A global two-dimensional hybrid simulation is carried out to study the evolution of the near-Earth plasma sheet. It is shown that reconnection X lines and plasmoids can be generated by diverging flows in the plasma sheet. These diverging flows can be caused by variations in the Maxwell stress due to variations of B_x and B_z components of the magnetic field outside the current sheet. In addition, the flow acceleration/deceleration in the plasma sheet can also be caused by variations in the local plasma mass density. Comparison runs have been made with a Harris model current sheet with zero B_z, and no evidence of reconnection is found. The results indicate that divergent plasma flow is a sufficient condition for reconnection even in a dissipation-less plasma. *INDEX TERMS:* 2788 Magnetospheric Physics: Storms and substorms; 2764 Magnetospheric Physics: Plasma sheet; 7835 Space Plasma Physics: Magnetic reconnection; 2744 Magnetospheric Physics: Magnetotail; 2753 Magnetospheric Physics: Numerical modeling; *KEYWORDS:* magnetic reconnection, divergent flow, magnetotail plasma sheet, hybrid simulation

Citation: Lin, Y., and D. W. Swift, Generation of near-Earth reconnection by divergent flows in the plasma sheet, *J. Geophys. Res.*, *107*(A11), 1373, doi:10.1029/2002JA009308, 2002.

1. Introduction

[2] The concept of magnetic reconnection was first brought into magnetospheric physics by *Dungey* [1961]. It is believed that the reconnection processes can take place at the magnetopause and in the distant magnetotail, leading to the transfer of the solar wind mass, momentum, and energy into the magnetosphere from the dayside magnetopause [e.g., *Russell and Elphic*, 1978] and the release of the energy and magnetic flux in the magnetotail [*Hones*, 1979; *Schindler*, 1975].

[3] The triggering mechanisms of geomagnetic substorms have been one of the most important problems in space plasma research. Various physical mechanisms have been proposed to explain the dynamics of the plasma sheet and its roles in the triggering of substorms. The near-Earth neutral line model [e.g., *Hones et al.*, 1973; *Hones*, 1984] suggests that a neutral line is formed between 10 and 20 R_E radial distance in the tail plasma sheet, and that the magnetic field reconnection resulted from tearing mode instability occurs at or very shortly after the expansion phase onset. Other observations of the near-tail reconnection [*Feldman et al.*, 1987; *Moldwin and Hughes*, 1992; *Cattell et al.*, 1992; *Nagai et al.*, 1998] indicate that the associated plasma sheet boundary layer is very different from that in the distant-tail reconnection, which often consists of a pair of quasi-steady slow shocks [e.g., *Feldman et al.*, 1984]. Although there has been no clear evidence that the near-Earth reconnection causes the expansion onset, the accelerated tailward and earthward flows associated with near-Earth reconnection have been observed between 20 and 30 R_E during substorm expansion [e.g., *Nagai et al.*, 1998], which indicate the existence of an X line between 20 and 30 R_E in the near-tail plasma sheet, consistent with the revised near-Earth neutral line model [*McPherron et al.*, 1993; *Baker*, 1996; *Birn and Hesse*, 1996]. Nevertheless, a large number of observations indicate that the substorm onset location lies at a distance of 10 R_E or less in the near-tail plasma sheet, inconsistent with the location of the near-Earth X line. The observations have also shown that the bursty bulk flows (BBFs) [*Angelopoulos et al.*, 1992], which are believed to be associated with the reconnection, cannot be one-to-one related to substorms. Other substorm models have also been proposed, including the new X line model [*Vasyliunas*, 1996], the fast flow breaking model [*Shiokawa et al.*, 1997], the cross-field current instability model [*Lui*, 1996], the ballooning instability model [*Roux et al.*, 1991], and other models [e.g., *Kan*, 1998; *Samson et al.*, 1996; *Rostoker*, 1996]. Although the formation of the near-tail X line may not be the direct cause of the substorm expansion onset, reconnection processes may be a part of the expansion onset process [e.g., *Baumjohann et al.*, 1999; *Ohtani et al.*, 1999].

[4] The physics of magnetic reconnection has been studied for decades on the bases of theoretical analysis [*Parker*, 1957; *Petschek*, 1964; *Vasyliunas*, 1975; *Hill*, 1975; *Axford*, 1984; *Sonnerup*, 1985; *White*, 1983; *Heyn et al.*, 1988; *Lin and Lee*, 1994], computer simulations [*Sato*, 1979; *Terasawa*, 1981; *Lee et al.*, 1985; *Swift*, 1986;

0148-0227/02/2002JA009308

Hoshino, 1987; *Krauss-Varban and Omidi*, 1995; *Lin and Swift*, 1996; *Lottermoser et al.*, 1998; *Hesse and Winske*, 1998; *Pritchett*, 2001; *Shay et al.*, 2001], and satellite observations [*Russell and Elphic*, 1978; *Sonnerup et al.*, 1981; *Feldman et al.*, 1984; *Smith et al.*, 1984; *Tsurutani et al.*, 1984]. The triggering and onset mechanisms of the reconnection in collision-less plasmas, however, are still unclear. It is more so for the near-Earth magnetotail because of the dipole geometry of the magnetic field lines: a necessary condition for the onset of the reconnection is the formation of a local thin current sheet whose thickness is on the order of electron inertial length, so that electron inertial effects or the anomalous resistivity associated with microinstabilities can trigger the reconnection in the current sheet. It has been proposed that the thin current sheet and reconnection can be generated following the disruption of the cross-tail current in the near-Earth region, by rarefaction waves down the tail [*Lui*, 1996]. In numerical simulations, the thin current sheet and the reconnection have been driven by convection electric field [e.g., *Lee et al.*, 1985; *Pritchett and Coroniti*, 1995; *Birn and Hesse*, 1996]. These simulations, however, do not include the dipole field in the domain and the resulting perturbing effects of the varying field line tension. Global MHD simulations [e.g., *Fedder et al.*, 1995] have shown the occurrence of the plasma sheet thinning and subsequent reconnection in the global evolution controlled by the solar wind. On the other hand, *Lee et al.* [1998] have proposed the formation of the thin current sheet by global entropy antidiffusion instability.

[5] In this paper, we propose an alternative mechanism for the generation of X lines and plasmoids in the near-Earth magnetotail: the reconnection can be produced by diverging flows in the local plasma sheet. Unlike a simple Harris sheet, an advantage of the magnetotail geometry of field lines is that it applies a finite magnetic tension force, or Maxwell stress, on the plasma sheet plasma. The variation of this force can effectively change the dynamics of the plasma sheet. We suggest that variations in the magnetic field can lead to variations in the Maxwell stress resulting in variations in acceleration in the plasma sheet. Local variations in plasma density can also result in variations in acceleration in the plasma sheet. Both effects can be very effective in causing divergence in plasma flux, which will result in thinning and depletion of the current sheet and eventual formation of reconnection X lines. In fact, observations suggested that the magnetotail may be commonly in nonequilibrium states. *Lyons et al.* [1997, 2001] reported the reduction in global convection and the substorm expansion onset occurred in association with a northward turning of the interplanetary magnetic field (IMF). The northward turning may leave the magnetosphere in a state of nonequilibrium. This suggests that the expansion phase onset is due to a change in external forcing, rather than an internally generated spontaneous event. Observations of the bursty bulk flow events showed strong fluctuations of the magnetic field and ion density in the plasma sheet [e.g., *Angelopoulos et al.*, 1992]. In the recent observation by *Sergeev et al.* [2001], sharp, significant variations of the plasma density and pressure were found at the flow burst onset. The variability of the observed convection also seems to indicate the pressure gradient and field line stress are often not in balance. The discussion in this paper focuses on the effects of such local transients, which do not require any plasma instability and have not been emphasized by previous simulations.

[6] This investigation uses a newly developed two-dimensional global hybrid code [*Swift and Lin*, 2001]. We use the hybrid code because MHD breaks down when ion gyroradii become comparable to the size scales of field variations, as it must in thin current layers and during reconnection. The hybrid code contains the physics of full kinetic ions, while the MHD does not treat the ions correctly. The hybrid code is also nearly dissipation-less. The simulation domain contains the nightside plasma regions in the noon–midnight meridian plane. The simulation model and the initial and boundary conditions are described in section 2. The results on the formation of reconnection X lines and the resulting kinetic structure of the plasma sheet are given in section 3. The conclusion is presented in section 4.

2. Simulation Model and Initial Conditions

[7] The two-dimensional hybrid simulation is carried out in the midnight meridian plane. The GSM coordinate system is used in this paper, with x pointing to the Sun and z pointing north. The y coordinate points from dawn to dusk. The center of the Earth is located at $(x, z) = (0, 0)$. The simulation domain extends from the surface of the Earth to $x = -35\ R_E$ in the antisunward direction and to $z = \pm 11\ R_E$ along the polar axes. Full ion kinetics is presented in a global-scale context, while the electrons are assumed to be a fluid. The code uses a generalized curvilinear coordinate system and was used by *Swift and Lin* [2001] for the simulation of the substorm onset and the generation of field-aligned currents in the plasma sheet. In the hybrid code, the magnetic field is advanced in time from Faraday's law. The electric field is calculated from the electron momentum equations, while the electron flow is calculated from Ampere's law. The ion particles are advanced in the electric and magnetic field.

[8] The fluid approximation is used in region with the geocentric distance $r < 6\ R_E$, where the plasma is not expected to have kinetic behavior. The plasma in this region of the plasmasphere and ionosphere is dense, so use of the fluid approximation results in an enormous computational saving. The code also allows the particle and fluid descriptions to occupy the same spatial volume [see also *Swift*, 1996].

[9] The initial magnetic field consists of a two-dimensional dipole plus a tail current sheet field, based upon a model of *Schindler* [1972], with a scale thickness of $1\ R_E$. The dipole field dominates the region with $x > -6\ R_E$. Beyond this distance the transition to the current sheet field is assumed, and the tail field dominates $x < -14\ R_E$. In a two-dimensional dipole, the field falls off as r^{-2}, instead of r^{-3} for a three-dimensional dipole. The dipole field strength at the Earth's surface is chosen as 2500 nT, so that the asymptotic lobe field B_0 in the magnetotail is chosen as 25 nT, comparable to observed values. Since the timing of the plasma sheet events of interests is largely determined by the asymptotic tail field, the times given should correspond to actual timings.

[10] The B_y component is initially set to zero. The initial ion particle density contains two populations. A cold population has a thermal velocity of 95 km/s. This fills the lobe regions of the magnetotail and the semicircular region surrounding the Earth at about 6 R_E. The density in the lobe is a uniform $400/R_E^2$, and the lobe ion inertial length is equal to 0.4 R_E. The lobe Alfvén speed is 660 km/s, and the ion plasma beta $\beta_0 = 0.01$ in the cold lobes. A hot population occupies the plasma sheet with a thermal velocity of 287 km/s. The density of this population is adjusted to maintain initial stress balance with the tail field in the z direction. A total of 2.2 million particles are loaded initially. The electron temperature is assumed to be zero for simplicity. The initial flow velocity is set to zero. The initial velocity distribution was assumed to be isotropic. For the cases shown in this paper, the pressure gradient in the x direction is much smaller compared with the Maxwell stress. At $t > 0$ the Maxwell stress is balanced by the momentum tensor associated with a finite earthward flow. We conjecture that the decrease in convection described by *Lyons et al.* [2001] leads to a decrease in the average convective flow stress. This leaves the plasma sheet at a state in which the sunward-directed Maxwell stress exceeds the antisunward stresses consisting of the pressure gradient and the residual flow stress. In our previous paper [*Swift and Lin*, 2001], we have also presented a case with a large pressure gradient in the x direction to balance the Maxwell stress. Since the effects shown in this paper are on transient timescales that can be applied to any slower timescale background conditions, the resulting perturbations are found not to depend on these different initial conditions. The influence of the convection speed V_x in the plasma sheet on the formation of the X line will be discussed in the next section. A key point is that the reconnection generated by the divergent flows can occur with or without an initial earthward flow.

[11] The boundary fields specify the tangential components of the electric field and the normal component of the magnetic field. The radial component of the magnetic field at the Earth's surface is assumed fixed to its dipole value. The normal component of B on the outer boundary is also assumed fixed. A dawn–dusk component of the electric field, E_y, is applied to the boundaries, except at the Earth's surface, where the y component was taken to be zero. The run that is featured in this paper was driven by the constant $E_{y0} = 0.023$ mV/m. The details of the corresponding particle boundary conditions are described fully by *Swift and Lin* [2001].

[12] In the following, velocities are presented in terms of the lobe Alfvén speed V_{A0}, the density is in units of the ion number density N_0 in the lobe, and the magnetic field intensity in units of the asymptotic lobe field B_0. For convenience, the time is expressed in units of seconds, and simulation distances are measured in Earth radii, R_E.

3. Simulation Results

[13] Three cases are shown in this paper. In case 1, a local enhancement in the Maxwell stress is imposed in the plasma sheet. Case 2 corresponds to an enhancement in the plasma density in the plasma sheet. Case 3 is run without these local variations and is shown for comparison. As shown in our previous simulation [*Swift and Lin*, 2001], in this last case a finite earthward flow V_x develops in the central plasma sheet. In the final equilibrium state the momentum stress $m_i N_0 V_x V_{z0}$ of the ion flow balances the Maxwell stress $B_{x0}B_{z0}/\mu_0$ from the lobes. Here, m_i is the ion mass, and V_{z0} is the z component flow velocity in the lobes.

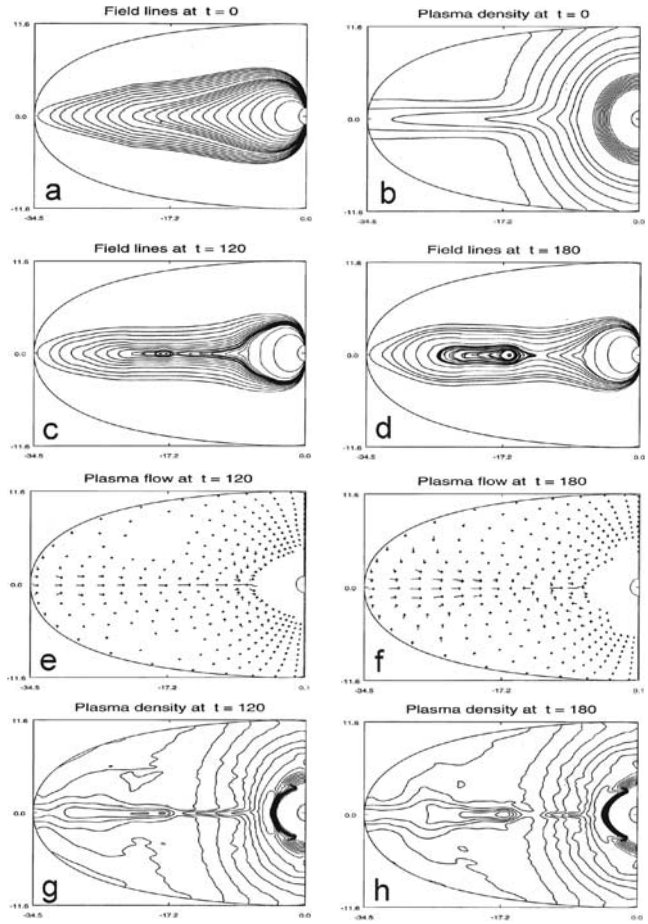

Figure 1. Results of case 1: initial magnetic field lines and ion number density contours (panels a and b) and the field lines, ion flow vectors, and ion density contours at $t = 120$ s (panels c, e, and g) and $t = 180$ s (panels d, f, and h). A magnetic field enhancement is applied to $x > -22$ R_E.

[14] In case 1, the x and z components of the current sheet magnetic field are assumed to increase by a factor of 2.75 in the plasma region with $x > -22$ R_E, across a width of 1 R_E. Note that the total magnetic field is the sum of the dipole field and the current sheet field. As a result, the product B_xB_z, the Maxwell stress, increases nearly by a factor of 4.3 in the region between $x \simeq -17$ to -22 R_E. During the simulation, the initial magnetic field is maintained at the boundary.

[15] The top two panels, a and b, in Figure 1 show the magnetic field lines and the ion number density contours initially at $t = 0$. An enhanced magnetic tension force is applied in $x > -22$ R_E. A typical current sheet-like ion density is assumed in the tail part of the magnetosphere, without a significant density gradient in the x direction. The reconnection is found to take place at $t \simeq 70$ s. Panels c, e, g in the left column of Figure 1 show the field lines, ion flow

vectors, and ion density contours at $t = 120$ s. Panels d, f, and h in the right column show the results at $t = 180$ s. At $t = 120$ s, an island of plasmoid appears in the field line plot, with an X line located at $x \simeq -16.5\ R_E$ in the central plasma sheet ($z \simeq 0$). The plasma flow speed V_x is enhanced on the earthward side of the X line due to the enhancement of the Maxwell stress. The enhanced earthward ion flux leads to a thin local current sheet, as seen from the density contour, and thus the X line.

[16] A case has been run for a simple Harris sheet with a zero B_z and the same cell sizes and ion scale lengths as in case 1. The initial current sheet was found to remain nearly unchanged, and no reconnection X line developed. Therefore the simulation code is sufficiently dissipationless that no reconnection occurs in a Harris sheet. In the hybrid simulation shown in case 1, the reconnection occurs when the current sheet is much thinner than the ion inertial length. Note that the hybrid code cannot solve the correct physics if the physical scale length is less than the grid spacing, which is on order of the ion inertial length. The actual mechanism that triggers the reconnection is beyond the scope of this study. In reality and in a calculation with the full ion and electron dynamics, the reconnection can be triggered by the anomalous resistivity associated with the electron dynamics [e.g., *Hoshino*, 1987]. Note that under divergent flow conditions, the density drops, which allows the electron inertial length to increase. The main point here is that the divergent flow forces smaller size scales, which also makes the electron inertia become important, and thus the occurrence of reconnection.

[17] In case 1, the thin current sheet and thus the reconnection occurs where the plasma flow is divergent. This diverging flow corresponds to a large gradient in V_x in the plasma sheet. Figure 2 shows the ion bulk flow component V_x near the central plasma sheet, i.e., along $z = 0$, as a function of x for $t = 0$ (dotted-dashed line), $t = 60$ s (dashed line), $t = 120$ s (dotted line), and $t = 180$ s (solid line). The normalization speed V_{A0} is the lobe Alfvén speed. At $t = 60$ s, a maximum gradient in V_x is seen around $x \simeq -18\ R_E$. The magnitude of V_x increases by a factor of 4 across this location. At $t = 120$ s, the location of the large V_x gradient has moved to $x \simeq -16.5\ R_E$ as the accelerated ion population carrying the field lines moved closer to the Earth under the large Maxwell stress cross the central current sheet. This location of the diverging V_x is where the X line appears, as seen in Figure 1.

[18] At $t = 180$ s, the location with the highly divergent V_x and thus the X line have moved to $X \simeq -12\ R_E$, as shown in Figures 1 and 2. The flow velocity V_x just behind the X line has been accelerated and turned tailward. Note that the boundary conditions on the fields have precluded antisunward flow out of the tail side boundary at $\sim -36\ R_E$. A large plasmoid occupies the region behind the X line, in which the magnetic field and the plasma density increase relative to the regions just earthward of the plasmoid. During the evolution of the plasma sheet, in addition to the Maxwell stress $\partial(B_xB_z/\mu_0)\partial z$ just across the thin current sheet that accelerates V_x, the force due to $-\partial(NV_x^2)/\partial x < 0$ acts to slow down this acceleration. Therefore the overall V_x is smaller than that is accelerated simply by the magnetic

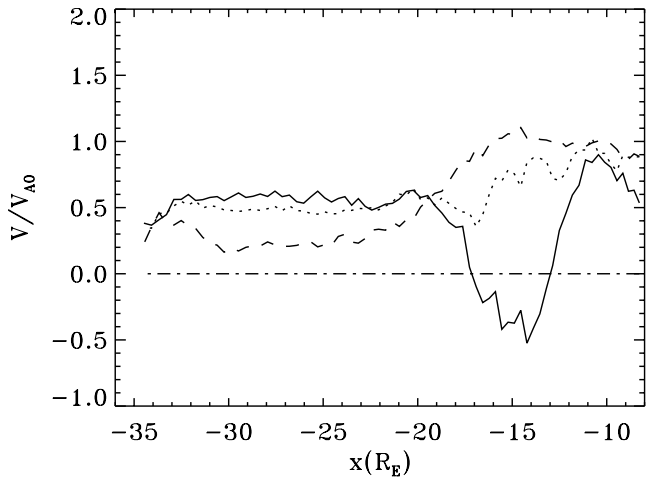

Figure 2. Ion bulk flow velocity V_x in case 1 along $z = 0$ as a function of x for $t = 0$ (dotted-dashed line), $t = 60$ s (dashed line), $t = 120$ s (dotted line), and $t = 180$ s (solid line).

force. The forces associated with pressures, $\partial P_\perp/\partial x$, $\partial[(P_\parallel - P_\perp)B_x^2/B^2]/\partial x$, and $\partial[(P_\parallel - P_\perp)B_xB_z/B^2]/\partial z$ are only significant near the X line.

[19] The divergent flow leads to a divergent ion flux for a nearly constant initial density in the central plasma sheet. The decrease in the local density, $\partial N/\partial t < 0$, is nearly balanced by $-\partial(NV_x)/\partial x$ according to the ion continuity equation. The region with the density depletion convects earthward with the flow. We can estimate how much increase in the Maxwell stress is required for the formation of a thin current sheet within the earthward convection time. In the reference frame that convects with the plasma sheet plasma, our simulation shows that the rate $\partial NV_x/\partial t$ is negligible at the center of the density depletion region before the X line forms, because of the decrease in the density and the increase in the flow speed. The momentum balance in the x direction can be written as

$$\frac{\partial}{\partial x}\left[\left(P_\perp + \frac{B^2}{2\mu_0}\right) + m_iNV_x^2 - \frac{B_x^2}{\mu_0} + \left(P_\parallel - P_\perp\right)\frac{B_x^2}{B^2}\right] + \frac{\partial}{\partial z}\left[m_iNV_xV_z - \frac{B_xB_z}{\mu_0} + \left(P_\parallel - P_\perp\right)\frac{B_xB_z}{B^2}\right] = 0 \qquad (1)$$

For the unperturbed state before the enhancement of local magnetic field, the total force is balanced with the presence of a uniform flow in the plasma sheet. In case 1, the pressure gradient force $\partial P_\perp/\partial x$ associated with the perturbed pressure is less than 5% of the Maxwell stress in the perturbed plasma sheet, and thus can be neglected for simplicity. The terms associated with the pressure anisotropy ($P_\parallel - P_\perp$) can also be neglected before the X line forms. The increase in the Maxwell stress mainly leads to an increased V_x in the plasma sheet. For the perturbed Maxwell stress and momentum, the second term in (1) associated with the z derivative across the current sheet can be approximately written as $[m_iN_0V_{z0}\Delta V_x/\Delta z - \Delta(B_{x0}B_{z0}/\mu_0)/\Delta z]$, where the subscript "0" represents the

quantities in the lobe, V_{z0} is the average inflow speed from the lobe, and ΔV_x is the change of V_x in the central plasma sheet. In the central plasma sheet, the magnetic field and thus the gradient forces associated with it are small. The term in (1) associated with the x derivative is dominated by the gradient in $m_i N V_x^2$ near $z = 0$. The increase in the Maxwell stress is then balanced by the change in plasma quantities as

$$\Delta\left(\frac{B_{x0}B_{z0}}{\mu_0}\right) \simeq \Delta z \frac{\partial}{\partial x}\left(m_i N V_x^2\right) + m_i N_0 V_{z0} \Delta V_x \tag{2}$$

Considering that the increase in the lobe magnetic field is through a distance Δx in the x direction, the rate of the relative change in Maxwell stress can be written as

$$\frac{1}{\Delta x}\frac{\Delta(B_{x0}B_{z0})}{B_{x0}B_{z0}} \simeq \frac{1}{N_0}\frac{\Delta z}{\Delta x}\frac{1}{V_{Ax0}V_{Az0}}\frac{\partial}{\partial x}\left(NV_x^2\right) + \frac{V_{z0}}{V_{Ax0}V_{Az0}}\frac{\Delta V_x}{\Delta x} \tag{3}$$

where $V_{Ax0} = B_{x0}/\sqrt{\mu_0 N_0}$ and $V_{Az0} = B_{z0}/\sqrt{\mu_0 N_0}$ are the components of the unperturbed Alfvén velocity in the lobe. On the other hand, from the continuity equation

$$\frac{\partial N}{\partial t} + \frac{\partial}{\partial x}(NV_x) = 0 \tag{4}$$

we have

$$\frac{\partial}{\partial x}\left(NV_x^2\right) = -2V_x\frac{\partial N}{\partial t} \tag{5}$$

and the rate of the velocity change along x

$$\frac{\Delta V_x}{\Delta x} \simeq \frac{\partial V_x}{\partial x} = -\frac{1}{N}\frac{\Delta N}{\Delta t} - \frac{V_x}{N}\frac{\Delta N}{\Delta x} \tag{6}$$

in the plasma sheet. Here $\Delta N < 0$ is the decrease in the local plasma sheet density due to the divergent flow, and $\Delta N/\Delta t \simeq \partial N/\partial t$ is the rate of the density change over a time period Δt. Inserting (5) and (6) into (3), and letting the average $V_{z0} \simeq 0.5\ V_{Az0}$, and the average V_x in the central plasma sheet $\simeq 0.5\ V_{Ax0}$, we have

$$\frac{1}{B_{x0}B_{z0}}\frac{\Delta(B_{x0}B_{z0})}{\Delta x} \simeq -\frac{1}{N_0 V_{Az0}}\frac{\Delta z}{\Delta x}\frac{\Delta N}{\Delta t} - \frac{0.5}{NV_{Ax0}}\frac{\Delta N}{\Delta t} - \frac{0.25}{N}\frac{\Delta N}{\Delta x} \tag{7}$$

In the simulation, the center of the region of divergent flow convects earthward with the flow, as shown in Figure 2. In order to obtain a significant density depletion of $\Delta N/N > 0.5$ within a convection distance of $\simeq 5\ R_E$, so that the thin current sheet and thus the X line can be formed, it is required that the rate of the density change

$$-\frac{\Delta N}{N}\frac{1}{\Delta t} > 0.5\frac{V_{Ax0}}{5R_E} \tag{8}$$

where the time interval $\Delta t \simeq 5\ R_E/V_{Ax0}$ for a convection speed $\sim V_{Ax0}$ leading the divergent flow region. Let the distance $\Delta x \simeq 5\ R_E$ associated with the x gradient of the Maxwell stress and $\Delta z \simeq 1\ R_E$ for the plasma sheet thickness. It is obtained from (7) that

$$\frac{1}{B_{x0}B_{z0}}\frac{\Delta(B_{x0}B_{z0})}{\Delta x} > \frac{0.1}{R_E}\left(\frac{N}{N_0}\frac{B_{x0}}{5B_{z0}} + 0.5\right) + \frac{0.025}{R_E} \tag{9}$$

Therefore, for an average density ratio between the central plasma sheet and the lobe of $N/N_0 \simeq 8$ and the ratio $B_{x0}/B_{z0} \sim 3$ in the simulation, the condition for the formation of a reconnection X line is estimated as

$$\frac{1}{B_{x0}B_{z0}}\frac{\Delta(B_{x0}B_{z0})}{\Delta x} > 0.6\ R_E^{-1} \tag{10}$$

In case 1, the left-hand side of (10) is nearly equal to $0.65\ R_E^{-1}$. Note that the minimum increase $\Delta(B_{x0}B_{z0})/B_{x0}B_{z0}$ required for the formation of X line can be smaller for a smaller Δx associated with the gradient in the Maxwell stress.

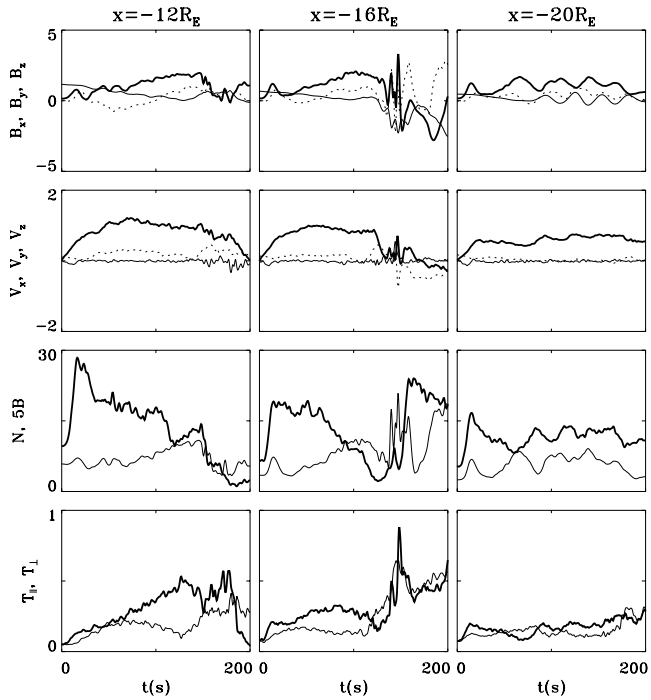

Figure 3. Time variation of B_x (thick solid line), B_y (dotted line), and B_z (thin solid line), V_x (thick solid line), V_y (dotted line), and V_z (thin solid line), N (thick), B (thin) multiplied by 5, $T_{\|}$ (thick), and $T_{\perp}$ (thin) along $z = 0$ in the central plasma sheet in case 1 at $x = -12\ R_E$ (left column), $-16\ R_E$ (middle), and $-20\ R_E$ (right).

[20] The top row of Figure 3 shows the time variation, from $t = 0$ to 200 s, of the magnetic field components B_x (thick solid line), B_y (dotted line), and B_z (thin solid line) at $x = -12\ R_E$ (left column), $-16\ R_E$ (middle column), and $-20\ R_E$ (right column) along $z \simeq 0$ in the central plasma sheet. The second row show of Figure 3 shows the time variation of ion bulk flow velocities V_x (thick solid line), V_y (dotted line), and V_z (thin solid line), the third row shows the ion number density N and the field strength B multiplied by 5, and the bottom row shows that parallel ion temperature $T_{\|}$ and perpendicular ion

temperature $T_\perp$. In Figure 3, the magnetic fields are normalized to the asymptotic lobe field B_0, the velocities are expressed in units of V_{A0}, N is in units of the lobe ion density N_0, and the temperatures are expressed in units of P_0/N_0, where $P_0 \equiv B_0^2/\mu_0$. At $x = -12\ R_E$, the earthward flow V_x rises from $t = 0$ in early times, and the density N increases sharply because of the rapid accumulation of the ions in front of the dipole region in response to the enhanced magnetic tension force. At $t > 25$ s, the density levels down at a value nearly twice as large as the initial one, corresponding to a much thinner current sheet. The B_z component also decreases. The value of V_x is leveled at $\sim V_{A0}$. The B_x component has increased from zero at $t = 0$ to small positive but wavy numbers. At $t > 60$ s, the center of the very thin current sheet is found to shift southward, so the original center at $z = 0$ is now located in the northern plasma sheet boundary layer, resulting in a positive B_x, an enhanced $T_\parallel/T_\perp$, and a reduced N.

[21] As the X line gets closer at $t > 100$ s, the B_y pattern associated with the Hall effect in the reconnection layer appears. Note that a quadrupolar structure of B_y is present in the symmetric reconnection layer, with $B_y > 0$ ($B_y < 0$) earthward (tailward) of the X line in the northern boundary layer and $B_y < 0$ ($B_y > 0$) earthward (tailward) of the X line in the southern boundary layer, corresponding to an electron sense magnetic field polarization in reconnection [e.g., *Lin*, 2001] and consistent with early predictions [e.g., *Sonnerup and Ledley*, 1979; *Terasawa*, 1983] and previous simulations [e.g., *Karimabadi et al.*, 1999; *Shay et al.*, 2001]. At $t > 100$ s for $x = -12\ R_E$, $B_y > 0$ (amplitude $\sim$25 nT) is present in the reconnection layer northward of the central plasma sheet and tailward of the X line, as shown in Figure 3. At $t \simeq 150$ s, the X line area has approached this location with $x = -12\ R_E$, as seen from the decreasing flow velocity and magnetic field and the increasing temperature.

[22] The passage of the X line area is seen more clearly at $x = -16\ R_E$ at $t > 120\ R_E$. Some significant oscillations in the magnetic field and the greatly reduced velocity are present, accompanied by the greatly increased temperature. Around the X line area, the thermal pressures $P_\parallel$ and $P_\perp$ increase significantly, and the forces associated with $P_\perp$ and the pressure anisotropy dominate the region near the X line, where the flow acceleration is not present. At later times with $t > 170$ s, the X line has moved to the earthward side of this location, and so a negative (tailward) V_x is present, as seen in the middle column of Figure 3. The density is also back up to the large value near the central plasma sheet. The negative B_x, however, indicates that this spatial location is now located in the boundary layer southward of the center of the plasma sheet. Correspondingly, $B_y > 0$ is reached for this location tailward of the X line. The location with $x = -20\ R_E$, on the other hand, is located in the plasmoid behind the X line during the entire period of $t > 70$ s. The B_x component is positive and $\gg B_z$ on average, while B_z is oscillating around a small value, indicating a thin current sheet embedded in the center of the evolving plasmoid. The V_x component at this location is directed earthward due to the dominant Maxwell stress from the lobes.

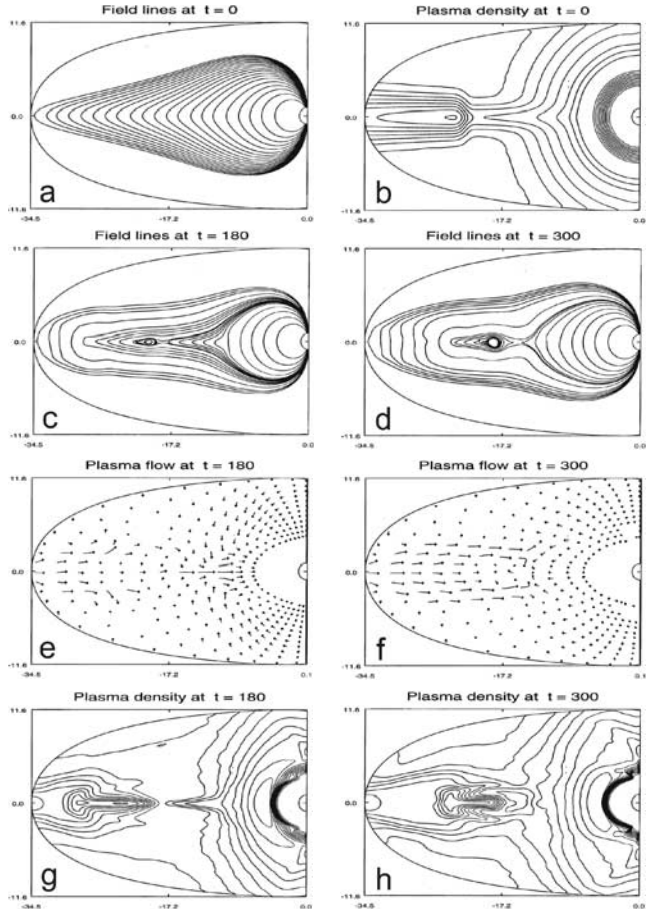

Figure 4. Initial state and results of case 2 at $t = 180$ and 300 s. Initially, a density enhancement is applied to $x < -22\ R_E$.

[23] We now show case 2, in which the reconnection X line is produced by changing the inertia of the plasma. In case 2, the initial number density of the hot ions (and correspondingly the electron density) in the plasma sheet is increased by a factor of 10 for $x < -22\ R_E$, while no enhancement in the Maxwell stress is applied. The temperature of the plasma sheet ions is assumed to decrease by a factor of 10 to maintain the total pressure balance in the direction normal to the current sheet at initial state. Similar to case 1, the x gradient of the thermal pressure is nearly zero in the tail plasma sheet. Figure 4 shows the initial state and the results of case 2 at $t = 180$ and 300 s.

[24] At $t = 180$ s, a reconnection X line has formed at $x \simeq -18\ R_E$. The flow speed on the tail side of the X line is found to be much smaller than that on the earthward side. Again, the X line exists in a thin current sheet, which is caused by the divergent flow in the plasma sheet. In this case, however, the divergent flow is only associated with $\partial V_x/\partial t \neq 0$ during the earthward acceleration of the flow. If initially a finite flow velocity is assumed as in the work of *Swift and Lin* [2001] according to the ($\mathbf{E} \times \mathbf{B}$) drift, the divergent flow and thus the X line will not be found. On the other hand, for case 1 the X line still exists even if the initial flow is

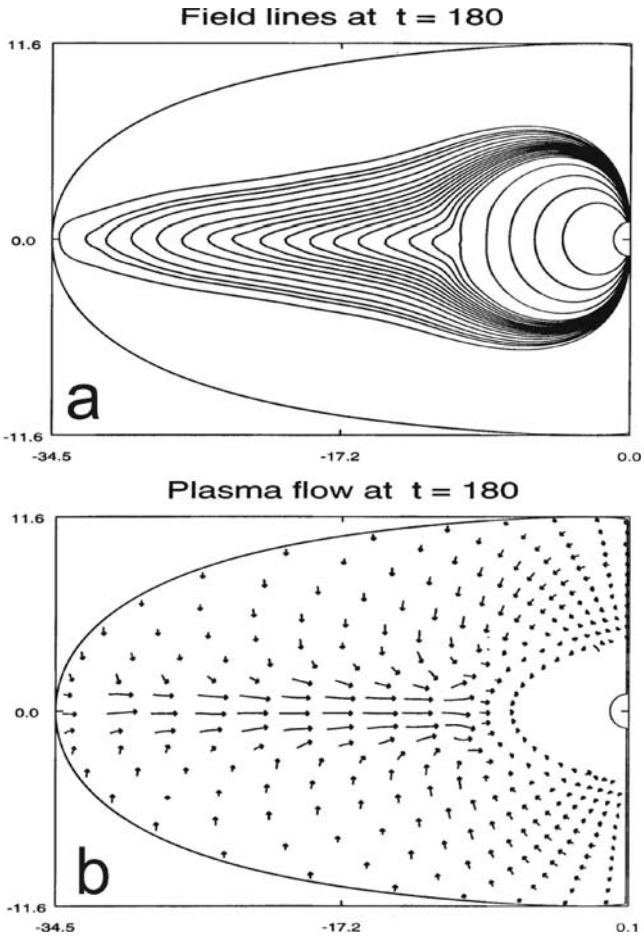

Figure 5. Results of case 3, without the magnetic field and density enhancement at t = 180 s.

imposed. In case 2, the large inertia due to the enhancement of N leads to the smaller $\partial V_x/\partial t$ and thus a smaller V_x in $x < -22\ R_E$. At t = 300 s, the X line moves to $x \simeq -15\ R_E$, and the plasmoid has grown larger. But the size of the plasmoid starts to decrease at $t > 40$ s. In a case similar to case 2 but with the initial N increased by a factor of 5 in $x < -22\ R_E$, the X line forms at $t \sim 180$ s but disappears at $t \sim 280$ s.

[25] A search has been conducted for the critical conditions for the existence of the near-tail reconnection. It is found that for cases similar to case 1, the X line can be formed if the Maxwell stress $B_{x0}B_{z0}/\mu_0$ across each lobe increases by a factor greater than 4.0, which roughly corresponds to the relative difference in the local V_x. For cases similar to case 2, the X line is present if the density increases by a factor greater than 4. In these critical cases, the X line exists only for a short period and then disappears.

[26] Finally, Figure 5 shows the results at t = 180 s of case 3, in which no local enhancements in magnetic field or density are applied in the plasma sheet. No reconnection event is observed in this case. The details of this case have been presented by *Swift and Lin* [2001]. Here we only mention that at t = 180 s a nearly constant $V_x \sim 0.7\ V_{A0}$ is developed along the tail plasma sheet. Due to the coupling between the current sheet and the dipole magnetic field, Small gradient forces in the $-x$ direction associated with the magnetic pressure and NV_x^2 are found to slow down the flow V_x.

4. Conclusion

[27] In summary, it is shown from a global hybrid simulation that reconnection X lines and plasmoids can be produced by diverging flows in the plasma sheet. These diverging flows can be caused by variations in the Maxwell stress cross the current sheet. In addition, the flow acceleration/deceleration in the plasma sheet can also be caused by variations in the local plasma mass density. The results indicate that divergent plasma flow is a sufficient condition for reconnection, and is very effective for the magnetotail field geometry. Our mechanism is demonstrated by a two-dimensional simulation. It should also be valid in the three-dimensional evolution of the plasma sheet.

[28] Although we have used a curvilinear coordinate system, which concentrates grid points in the plasma sheet, our resolution is still not fine enough to resolve the electron inertial length. However, we do observe the magnetic field structure down to the resolution of the grid. Furthermore, we observe very low plasma densities to develop in the region of fine structure. Although we have not proven it, there seems to be no reason to believe that this process of current sheet thinning and electron inertial length increase will not continue until conditions for reconnection are satisfied. The reconnection process may be likened to vacuum field line connection of the type that occurs when two bar magnets of opposite polarity are brought together. Such a process does not require any plasma instability. Even though our code does not simulate the exact microphysics for the initiation of reconnection, it does show that divergent flow is an important, and perhaps dominant, agent for the initiation of reconnection in the magnetosphere.

[29] The simulations presented were initiated with a plasma field configuration in which the field line tension forces exceeded the x component of the pressure gradient. Reconnection is generally believed to accompany the substorm expansion phase. *Lyons et al.* [1997, 2001] maintain the substorm expansive phase follows from a northward turning of the IMF and a decrease in convection. Our view is that during the growth phase when there is strong convection and plasma sheet thinning, the tail field is being stretched. When convection ceases, the magnetotail is left in a state where the Maxwell stresses exceed the pressure gradient forces and cause earthward acceleration of plasma.

[30] The simulations also assumed field and plasma density variations. It appears in the growth phase accompanied by enhanced levels of BBF activity [*Lyons et al.*, 1999; *Angelopoulos et al*, 1992]. This activity is characterized by irregularities in plasma density [*Sergeev et al.*, 2001] and significant field variations. Variation of plasma sheet mass density can also be caused by variations in ion composition. The central point of this paper is that reconnection accompanyin g substorm expansion may be due flow divergence of magnetotail flows that accompany

the substorm expansion and that there is a reasonable probability for the existence of conditions for divergent flow.

[31] **Acknowledgments.** This work was supported by NASA grant NAG5-8081 and NSF grant ATM-9805550 to Auburn University and NSF grant 008754 at the University of Alaska. Computer resources were provided by the National Partnership for Advanced Computational Infrastructure, the Arctic Region Supercomputer Center, and the Alabama Supercomputer Center.

References

Angelopoulos, V., W. Baumjohann, C. F. Kennel, F. V. Coroniti, M. G. Kivelson, R. Pellat, R. J. Walker, H. Luhr, and G. Paschmann, Bursty bulk flows in the inner central plasma sheet, *J. Geophys. Res.*, *97*, 4027, 1992.

Axford, W. I., Magnetic field reconnection, in *Magnetic Reconnection in Space and Laboratory Plasmas, Geophys. Monogr.*, vol. 30, edited by E. W. Hones Jr., p. 1, AGU, Washington, D. C., 1984.

Baker, D. N., Magnetic reconnection during magnetospheric substorms, in *Proceedings of the Third International Conference on Substorms (ICS-3), Versailles, France, ESA SP*, vol. 389, p. 365, 12–17 May 1996.

Baumjohann, W., M. Hesse, S. Kokubun, T. Mukai, and T. Nagai, Substorm dipolarization and recovery, *J. Geophys. Res.*, *104*, 1999.

Birn, J., and M. Hesse, Details of current disruption and diversion in simulations of magnetotail dynamics, *J. Geophys. Res.*, *101*, 15,345, 1996.

Cattell, C. A., C. W. Carlson, W. Baumjohann, and H. Luhr, The MHD structure of the plasma sheet boundary, 1, Tangential momentum balance and consistency with slow mode shocks, *Geophys. Res. Lett.*, *19*, 2083, 1992.

Dungey, J. W., Interplanetary magnetic field and the auroral zones, *Phys. Rev. Lett.*, *6*, 47, 1961.

Fedder, J. A., S. P. Slinker, J. G. Lyon, and R. D. Elphinstone, Global numerical simulation of the growth phase and the expansion onset for a substorm observed by Viking, *J. Geophys. Res.*, *100*, 19,083, 1995.

Feldman, W. C., et al., Evidence for slow-mode shock in the deep geomagnetic tail, *Geophys. Res. Lett.*, *11*, 599, 1984.

Feldman, W. C., R. L. Tokas, J. Birn, E. W. Hones Jr., S. J. Bame, and C. T. Russell, Structure of a slow mode shock observed in the plasma sheet boundary layer, *J. Geophys. Res.*, *92*, 83, 1987.

Hesse, M., and D. Winske, Electron dissipation in collisionless magnetic reconnection, *J. Geophys. Res.*, *103*, 26,479, 1998.

Heyn, M. F., H. K. Biernat, R. P. Rijnbeek, and V. S. Semenov, The structure of reconnection layer, *J. Plasma Phys.*, *40*, 235, 1988.

Hill, T. W., Magnetic merging in a collisionless plasma, *J. Geophys. Res.*, *80*, 4689, 1975.

Hones, E. W., Jr., Transient phenomena in the magnetotail and their relation to substorms, *Space Sci. Rev.*, *23*, 393, 1979.

Hones, E. W., Jr., Plasma sheet behavior during substorms, in *Magnetic Reconnection in Space and Laboratory Plasmas*, edited by E. W. Hones Jr., p. 178, AGU, Washington, D. C., 1984.

Hones, E. W., Jr., J. R. Asbridge, S. J. Bame, and S. Singer, Substorm variations of the magnetotail plasma sheet from X −6Re to X −60Re, *J. Geophys. Res.*, *78*, 109, 1973.

Hoshino, M., The electrostatic effect for the collisionless tearing mode, *J. Geophys. Res.*, *92*, 7368, 1987.

Kan, J. R., A globally integrated substorm model: Tail reconnection and magnetosphere–ionosphere coupling, *J. Geophys. Res.*, *103*, 11,787, 1998.

Karimabadi, H., D. Krauss-Varban, N. Omidi, and H. X. Vu, Magnetic structure of the reconnection layer and core field generation in plasmoids, *J. Geophys. Res.*, *104*, 12,313, 1999.

Krauss-Varban, D., and N. Omidi, Large-scale hybrid simulations of the magnetotail during reconnection, *Geophys. Res. Lett.*, *22*, 3271, 1995.

Lee, L. C., Z. F. Fu, and S.-I. Akasofu, A simulation study of the forced reconnection processes and magnetospheric storms and substorms, *J. Geophys. Res.*, *90*, 10,896, 1985.

Lee, L. C., L. Zhang, A. Otto, G. S. Choe, and H. J. Cai, Entropy antidiffusion instability and formation of a thin current sheet during geomagnetic substorm, *J. Geophys. Res.*, *103*, 29,419, 1998.

Lin, Y., Global hybrid simulation of the magnetopause reconnection layer and associated field-aligned currents, *J. Geophys. Res.*, *106*, 25,451, 2001.

Lin, Y., and L. C. Lee, Structure of reconnection layers in the magnetosphere, *Space Sci. Rev.*, *65*, 59, 1994.

Lin, Y., and D. W. Swift, A two-dimensional hybrid simulation of the magnetotail reconnection layer, *J. Geophys. Res.*, *101*, 19,859, 1996.

Lottermoser, R. F., M. Scholer, and A. P. Matthews, Ion kinetic effects in magnetic reconnection: Hybrid simulations, *J. Geophys. Res.*, *103*, 4547, 1998.

Lui, A. T. Y., Current disruption in the Earth's magnetosphere: Observations and models, *J. Geophys. Res.*, *101*, 13,067, 1996.

Lyons, L. R., G. T. Blanchard, J. C. Samson, R. P. Lepping, T. Yamamoto, and T. Mretto, Coordinated observations demonstrating external substorm triggering, *J. Geophys. Res.*, *102*, 27,039, 1997.

Lyons, L. R., T. Magai, G. T. Blachard, J. C. Samson, T. Yamamoto, T. Mukai, A. Sishida, and S. Kokubun, Association between Geotail plasma flows and auroral poleward boundary intensifications observed by CANOPUS photometers, *J. Geophys. Res.*, *104*, 4485, 1999.

Lyons, L. R., J. M. Ruohoniemi, and G. Lu, Substorm-associated change in large-scale convection during the November 24, 1996 Geospace Environment Modeling event, *J. Geophys. Res.*, *106*, 397, 2001.

McPherron, R. L., V. Angelopoulos, D. N. Baker, and E. W. Hones Jr., Is there a near-Earth neutral line?, *Adv. Space Res.*, *13*(4), 173, 1993.

Moldwin, M. B., and W. J. Hughes, On the formation and evolution of plasmoids: A survey of ISEE 3 Geotail data, *J. Geophys. Res.*, *97*, 19,259, 1992.

Nagai, T., M. Fujimoto, Y. Saito, S. Machida, T. Terasawa, R. Nakamura, T. Yamamoto, T. Mukai, A. Nishida, and S. Kokubun, Structure and dynamics of magnetic reconnection for substorm onsets, with Geotail observations, *J. Geophys. Res.*, *103*, 4419, 1998.

Ohtani, S., F. Creutzberg, T. Mukai, H. Singer, A. T. Y. Lui, M. Nakamura, P. Prikryl, K. Yumoto, and G. Rostoker, Substorm onset timing: The December 31, 1995 event, *J. Geophys. Res.*, *104*, 22,713, 1999.

Parker, E. N., Sweet's mechanism for merging magnetic fields in conducting fluids, *J. Geophys. Res.*, *62*, 509, 1957.

Petschek, H. E., Magnetic field annihilation, in *AAS–NASA Symposium on the Physics of Solar Flares, NASA Spec. Publ.*, vol. 50, pp. 425–439, 1964.

Pritchett, P. L., Geospace Environment Modeling magnetic reconnection challenge: Simulations with a full particle electromagnetic code, *J. Geophys. Res.*, *106*, 3783, 2001.

Pritchett, P. L., and F. V. Coroniti, Formation of thin current sheets during plasma sheet convection, *J. Geophys. Res.*, *100*, 23,551, 1995.

Rostoker, G., Phenomenology and physics of magnetospheric substorms, *J. Geophys. Res.*, *101*, 12,995, 1996.

Roux, A., S. Perraut, P. Robert, A. Morane, A. Pederson, A. Korth, G. Kremser, B. Aparicio, D. Rodgers, and R. Pellinen, Plasma sheet instability related to the westward traveling surges, *J. Geophys. Res.*, *96*, 17,697, 1991.

Russell, C. T., and R. C. Elphic, Initial ISEE magnetometer results: Magnetopause observations, *Space Sci. Rev.*, *22*, 691, 1978.

Samson, J. C., et al., Substorm intensifications and resistive shear flow-ballooning instabilities in the near-Earth magnetotail, in *Proceedings of the Third International Conference on Substorms (ICS-3),Versailles, France, ESA SP*, vol. 389, p. 399, 12–17 May 1996.

Sato, T., Strong plasma acceleration by slow shocks resulting from magnetic reconnection, *J. Geophys. Res.*, *84*, 7177, 1979.

Schindler, K., A self-consistent theory of the tail of the magnetosphere, in *Earth's Magnetospheric Processes*, edited by B. M. McCormac, p. 200, D. Reidel, Norwell, Mass., 1972.

Schindler, K., Plasma and fields in the magnetospheric tail, *Space Sci. Rev.*, *17*, 589, 1975.

Sergeev, V. A., M. V. Kubyshkina, K. Liou, P. T. Newell, G. Parks, R. Nakamura, and T. Mukai, Substorm and convection bay compared: Auroral and magnetotail dynamics during convection bay, *J. Geophys. Res.*, *106*, 18,843, 2001.

Shay, M. A., J. F. Drake, B. N. Rogers, and R. E. Denton, Alfvénic collisionless magnetic reconnection and the Hall term, *J. Geophys. Res.*, *106*, 3759, 2001.

Shiokawa, K., W. Baumjohann, and G. Haerendel, Braking of high-speed flows in the near-Earth tail, *Geophys. Res. Lett.*, *24*, 1179, 1997.

Smith, E. J., J. A. Slavin, B. T. Tsurutani, W. C. Feldman, and S. J. Bame, Slow mode shocks in the Earth's magnetotail: ISEE-3, *Geophys. Res. Lett.*, *11*, 1054, 1984.

Sonnerup, B. U. O., Magnetic field reconnection in cosmic plasmas, in *Unstable Current Systems and Plasma Instabilities in Astrophysics*, edited by M. R. Kundo and G. D. Holman, D. Reidel, Norwell, Mass., 1985.

Sonnerup, B. U. O., and B. G. Ledley, OGO 5 magnetopause structure and classical reconnection, *J. Geophys. Res.*, *84*, 399, 1979.

Sonnerup, B. U. O., G. Paschmann, I. Papamastorakis, N. Sckopke, G. Haerendel, S. J. Bame, J. R. Asbridge, J. T. Gosling, and C. T. Russell, Evidence for magnetic reconnection at the Earth's magnetopause, *J. Geophys., Res.*, *86*, 10,049, 1981.

Swift, D. W., Numerical simulations of tearing mode instabilities, *J. Geophys. Res.*, *91*, 219, 1986.

Swift, D. W., Use of a hybrid code for a global-scale plasma simulation, *J. Comput. Phys.*, *126*, 109, 1996.

Swift, D. W., and Y. Lin, Substorm onset viewed by a two-dimensional, global-scale hybrid code, *J. Atmos. Sol. Terr. Phys.*, *63*, 683–704, 2001.
Terasawa, T., Numerical study of explosive tearing mode instability in one-component plasma, *J. Geophys. Res.*, *86*, 9007, 1981.
Terasawa, T., Hall current effect on tearing mode instability, *Geophys. Res. Lett.*, *10*, 475, 1983.
Tsurutani, B. T., et al., Magnetic structure of the distant Geotail from 60 to 220Re: ISEE-3, *Geophys. Res. Lett.*, *11*, 1, 1984.
White, R. B., Resistive instabilities and field line reconnection, in *Handbook of Plasma Physics, Vol. I, Basic Plasma Physics*, edited by A. A. Galeev and R. N. Sudan, p. 611, North-Holland, New York, 1983.
Vasyliunas, V. M., Theoretical models of magnetic field line merging, 1, *Rev. Geophys.*, *13*, 303, 1975.
Vasyliunas, V. M., The substorm as a flux transfer process, *Abstracts of the Third International Conference on Substorms* (*ICS-3*), Versailles, France, SP, vol. 389, p. 169, 12–14 May 1996.

Y. Lin, Physics Department, Auburn University, 206 Allison Laboratory, Auburn, AL 36849-5311, USA. (ylin@physics.auburn.edu)
D. W. Swift, Geophysical Institute, University of Alaska, Fairbanks, AK 99775-7320, USA. (swift@gi.alaska.edu)